

AD-A198 870

DTIC FILE COPY
4

SECURITY CLASSIFICATION OF THIS PAGE (When Data Entered)

REPORT DOCUMENTATION PAGE		READ INSTRUCTIONS BEFORE COMPLETING FORM
1. REPORT NUMBER ONR NR 659-819/11/87	2. GOVT ACCESSION NO.	3. RECIPIENT'S CATALOG NUMBER
4. TITLE (and Subtitle) THE INFRARED MULTIPHOTON DISSOCIATION OF ETHYL AND METHYL ACETATE		5. TYPE OF REPORT & PERIOD COVERED TECHNICAL REPORT
		6. PERFORMING ORG. REPORT NUMBER
7. AUTHOR(s) Eric J. Hintska, Alec M. Wodtke and Yuan T. Lee		8. CONTRACT OR GRANT NUMBER(s) N00014-83-K-0069 NR 659-819
9. PERFORMING ORGANIZATION NAME AND ADDRESS Professor Yuan T. Lee Dept. of Chemistry, Univ. of California Berkeley, California 94720		10. PROGRAM ELEMENT, PROJECT, TASK AREA & WORK UNIT NUMBERS
11. CONTROLLING OFFICE NAME AND ADDRESS Dr. Richard S. Miller, Office of Naval Research Dept. of the Navy, Office of Naval Research 800 N. Quincy Street, Arlington, VA 22217		12. REPORT DATE November 10, 1987
14. MONITORING AGENCY NAME & ADDRESS (if different from Controlling Office) Office of Naval Research-Resident Representative UCB Residency, Richmond Field Station University of Calif., Berkeley, CA 94720		13. NUMBER OF PAGES 45
16. DISTRIBUTION STATEMENT (of this Report) submitted to Journal of Physical Chemistry unlimited		15. SECURITY CLASS. (of this report) Unclassified
		15a. DECLASSIFICATION/DOWNGRADING SCHEDULE
17. DISTRIBUTION STATEMENT (of the abstract entered in Block 20, if different from Report)		DTIC ELECTE S AUG 04 1988 D H
18. SUPPLEMENTARY NOTES None		
19. KEY WORDS (Continue on reverse side if necessary and identify by block number) Infrared multiphoton dissociation, concerted unimolecular reactions, ethyl acetate, methyl acetate, reaction barriers, RRKM theory, molecular beams, ethers.		
20. ABSTRACT (Continue on reverse side if necessary and identify by block number) (See reverse side)		

20. Abstract

The collisionless decomposition of ethyl and methyl acetate was investigated using IR multiphoton dissociation. With a fluence of 40 J/cm^2 , Ethyl acetate gave 97 percent concerted decomposition producing ethylene and acetic acid, the latter of which underwent significant secondary decomposition to ketene and water. Simple bond rupture producing ethyl radical and CH_3CO_2 , which completely decomposed to CH_3 and CO_2 , accounted for the remaining reaction products. Methyl acetate underwent concerted reaction to produce methanol and ketene, and simple bond rupture to form CH_3 and CH_3CO_2 , in near equal amounts. All of the concerted reactions released more than half ($\sim 20 \text{ kcal/mol}$) of the exit channel barrier into translational energy. Using the branching ratio between the two channels and the translational energy distribution of the simple bond rupture channel, the barrier for concerted reaction in methyl acetate was determined to be $69 \pm 3 \text{ kcal/mol}$.



Accession For	
NTIS	SPART
PTIC	TAN
Unpublished	
JULY 1981	
FBI - WASHINGTON	
LAW ENFORCEMENT	
LITERATURE	
ACADEMIC	
LAW LIBRARY	
DRAFT	
A-1	

The Infrared Multiphoton Dissociation of
Ethyl and Methyl Acetate

Eric J. Hints, Alec M. Wodtke,* and Yuan T. Lee

Materials and Molecular Research Division,
Lawrence Berkeley Laboratory and
Department of Chemistry, University of California
Berkeley, California 94720 USA

Abstract.

The collisionless decomposition of ethyl and methyl acetate was investigated using IR multiphoton dissociation. With a fluence of 40 J/cm², ethyl acetate gave 97 percent concerted decomposition producing ethylene and acetic acid, the latter of which underwent significant secondary decomposition to ketene and water. Simple bond rupture producing ethyl radical and CH₃CO₂, which completely decomposed to CH₃ and CO₂, accounted for the remaining reaction products. Methyl acetate underwent concerted reaction to produce methanol and ketene, and simple bond rupture to form CH₃ and CH₃CO₂, in near equal amounts. All of the concerted reactions released more than half (~20 kcal/mol) of the exit channel barrier into translational energy. Using the branching ratio between the two channels and the translational energy distribution of the simple bond rupture channel, the barrier for concerted reaction in methyl acetate was determined to be 69±3 kcal/mol.

*Present Address: Max Planck Institut für Strömungsforschung, Bunsenstr.
10, Göttingen D-3400, West Germany.

Introduction.

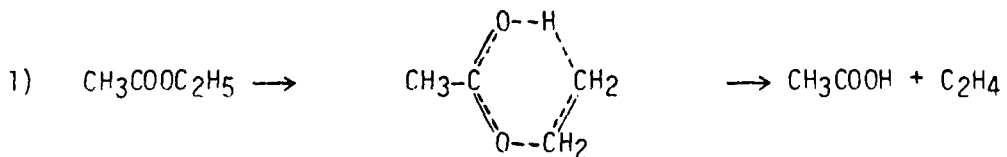
Since its discovery in the early 1970s, the phenomenon of multiphoton dissociation (MPD) has generated an intense amount of interest.¹ Much early work focused on isotope separation and exploring the possibility of bond selective chemistry by exciting a local mode in a polyatomic molecule. Although rapid intramolecular vibrational relaxation prevents true bond selective fission,² this allows MPD to be used as a method for performing essentially "thermal" experiments in the collisionless environment of a molecular beam.^{3,4}

The process of MPD can be roughly divided into three regions.⁵ In the lowest region the molecules are excited through discrete rovibrational levels by intensity dependent resonant absorption until the vibrational density of states becomes large enough for energy randomization to compete with absorption. In this "quasicontinuum" the molecules are pumped to higher and higher levels by stepwise incoherent excitation. Once the molecules are excited over the dissociation barrier, decomposition competes with continued up-pumping. The laser intensity determines how high the molecules are excited during the laser pulse before they dissociate, as long as the fluence is sufficient to dissociate most of the molecules in the quasicontinuum. If there is more than one possible decay channel at reasonably low energies, competition between the different pathways may be observed.^{3,4} At high levels of excitation, vibrational energy is randomized on a picosecond timescale and statistical methods such as RRKM theory can be used to calculate the unimolecular rate constants. For simple bond rupture reactions, where there is no exit channel barrier, RRKM theory

can be easily extended to predict the translational energy distribution of the products, allowing the average energy of the dissociating molecules to be determined. Using the translational energy distribution and the endoergicity of one channel and the branching ratio between two competing channels, we have shown that it is possible to find the dissociation barrier of the other channel.⁴

This is especially relevant to cases where a concerted reaction competes with simple bond rupture. In a concerted reaction, bonds are broken and formed simultaneously, often through a cyclic transition state followed by a large release of translational energy. As part of an effort to understand the dynamics of translational energy release from different types of transition states, we have recently completed a molecular beam IRMPD study of various nitro compounds and esters.^{4,6}

Ethyl acetate is well known to undergo reaction through a six membered transition state to form ethylene and acetic acid:



This reaction is endothermic by 12 kcal/mol, but the activation energy has been determined to be 48.0 kcal/mol⁷ leaving an exit channel barrier of about 36 kcal/mol. While a few MPD studies of ethyl acetate have been performed in gas cells^{8,9} confirming the occurrence of reaction (1), there has been no determination of the fraction of energy released into translation or the internal degrees of freedom. In comparison there have

been very few studies of methyl acetate thermolysis. Carlsen and coworkers determined by isotope labeling and mass spectrometry that the major reaction at medium temperatures (~1000 K) was methyl group migration from one oxygen atom to the other, with ketene and methanol also produced in low yield.¹⁰ In a recent high temperature (1400–1800 K) reflected shock wave study, Sulzmann and coworkers found only CO₂ and methyl radicals, though they did not monitor other possible channels.¹¹ Energy level diagrams including possible decomposition products for ethyl and methyl acetate are shown in figures 1 and 2. The primary decomposition channels which we observed are indicated by dashed lines.

Experimental.

The rotating source molecular beam translational energy spectrometer has been previously described in detail.¹² Briefly, helium was bubbled through the liquid under study and passed through a 125 μm nozzle creating a supersonic expansion with a mean velocity of 1.3×10^5 cm/sec (ethyl acetate) or 1.6×10^5 cm/sec (methyl acetate) and a full width at half maximum (FWHM) spread of about 10 percent. The acetates were held in a bubbler at 0°C with a total backing pressure of 350 Torr. The nozzle was heated to 250°C to eliminate cluster formation and improve absorption of IP radiation by the molecules. After passing through two collimating skimmers in differentially pumped regions which defined it to a 1.5° FWHM angular spread, the molecular beam was crossed with the focused output of a Gentec CO₂ laser operating on the P(22) line of the 9.6 μm branch (1045 cm^{-1}) with a fluence of about 40 J/cm². The entire source rotates about the interaction region to allow data collection at source to detector angles

of 0° to 90° . After passing through two more regions of differential pumping, a small ($\sim 1.5^\circ$) angular fraction of the MPD fragments was detected by a quadrupole mass spectrometer using an electron impact ionizer and ion counting techniques. The detector output was sampled by a multichannel scaler, triggered by the laser, for time-of-flight (TOF) measurements of product velocity distributions. Most of the data were taken at a source to detector angle of 20° , with 40,000 to 1,000,000 laser shots being required to achieve good signal to noise at different masses.

Results and Analysis.

The data was analyzed with forward convolution techniques¹³ to determine the translational energy release. An assumed product translational energy probability distribution ($P(E_T)$) for a particular reaction channel is converted to a center of mass (c.m.) velocity flux distribution for one of the pair of products related by conservation of linear momentum. This c.m. velocity distribution is added vectorially to the beam velocity (obtained by beam TOF measurements using a spinning slotted disk) and transformed to a lab velocity flux distribution for a given source to detector angle using the appropriate Jacobian factor. Experimental parameters are averaged over, principally the beam velocity spread, but also the finite length of the ionizer and the spread in beam angles. The resulting lab velocity distribution is converted to a theoretical TOF spectrum which can be compared to the experimental data. The $P(E_T)$ is then adjusted until the theoretical and experimental TOF spectra match. Secondary dissociation is modeled in an analogous way though with a more complicated algorithm.¹⁴ Essentially, a primary c.m. flux

distribution is converted to a density distribution in the primary reactant c.m. coordinates, then using a second $P(E_T)$ a secondary flux distribution is calculated from the primary one. From this secondary distribution the contributions at a given angle are calculated, using the correct transformation factors.

A). Ethyl Acetate

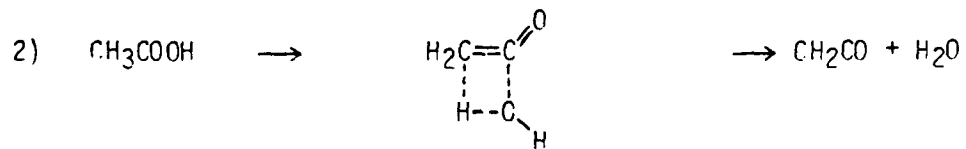
Signal from MPD of ethyl acetate was observed at mass to charge ratios (m/e) of 13-18, 26-31, 42-45, and 59, but not at $m/e = 60$. A chart with all the detected ion masses, their corresponding neutral fragments, the reaction channel to which they have been assigned, and the relevant figure, is shown in table 1. As expected, reaction (1) producing acetic acid and ethylene was the dominant channel. The peaks in the $m/e = 26$ and 45 TOF spectra in figure 3 are from ethylene and the momentum matched acetic acid fragment respectively. Ethylene also appears as the parent ion ($m/e = 28$) and at several other masses, but the acetic acid produces no signal at $m/e = 60$ though it appears at almost all the lower daughter ion masses including $m/e = 59$. This absence of the parent ion is not surprising, as it has been previously found that highly vibrationally excited species undergo extensive fragmentation in the electron bombardment ionizer and analysis must be based on the detection of daughter ions.¹⁵

The $P(E_T)$'s derived from the $m/e = 26$ and 45 spectra are shown in figure 4 and the fits to the data are shown in figure 3. The $P(E_T)$ of ethylene peaks at 19 kcal/mol and releases an average of 21.7 kcal/mol into translation. For a process producing two fragments both of which are detected, the $P(E_T)$ derived from one should fit the other, but this is not

the case for acetic acid recoiling from ethylene as can be seen in figure 3, bottom, with a dotted line showing the acetic acid data fit with the $P(E_T)$ derived from the ethylene data. The peak and the fast edge match well (substantiating the identification of this channel) but the $P(E_T)$ derived from the ethylene data predicts considerably more slow acetic acid. The main difference between this $P(E_T)$ and that derived from the acetic acid data occurs at energies below 10 kcal/mol, as shown in figure 4.

An explanation of this comes from the fact that acetic acid may undergo secondary decomposition, with or without the absorption of more photons. Though not rigorously true for IRMPD where the molecules dissociate from a considerable range of energy levels, molecules releasing a smaller amount of the energy of an exit channel barrier into translation should have, on the average, more internal energy and thus be more likely to undergo secondary dissociation.

The secondary dissociation products of acetic acid are ketene and water produced by reaction (2) through a four-membered transition state, and their



TOF spectra are shown in figure 5. These results were confirmed by MPD experiments on acetic acid¹⁶ and are in agreement with previous thermal studies.^{7,17}

Since it was found that 67 percent of the acetic acid produced underwent secondary decomposition (vide infra), neither the $P(E_T)$ derived

from ethylene or acetic acid was suitable for use as the primary $P(E_T)$ for acetic acid which eventually decomposed. This problem was resolved by taking the $P(E_T)$ for ethylene and subtracting 33 percent of the $P(E_T)$ for acetic acid (both initially normalized to unity), which represents the surviving acetic acid. The resulting primary $P(E_T)$ corresponds to the shaded area in figure 4, and though similar in shape to that for ethylene, contains a higher contribution from lower translational energies as these preferentially underwent secondary decomposition. The $P(E_T)$ for secondary dissociation is shown in figure 6 and the fits to the data are shown in figure 5. The peak of the $P(E_T)$ is at 25 kcal/mol with an average of 23.7 kcal/mol released to translation, though these numbers for secondary dissociation are inherently more uncertain. There was no evidence for any secondary dissociation of ethylene or any further dissociation of ketene.

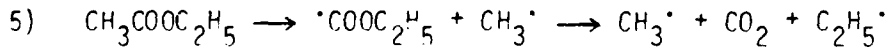
In addition to the concerted reaction pathway there was evidence for another reaction occurring. Data at $m/e = 15$ and 44 (shown in figure 7) could not be fit with reactions (1) and (2). The mass 15 TOF spectrum shows extremely fast signal and that at mass 44 is very broad, with signal appearing at faster and slower arrival times than would be expected from acetic acid. If the weakest bond in ethyl acetate, between one O atom and the ethyl group, broke to produce the acetoxy radical ($\text{CH}_3\text{COO}^\cdot$) and an ethyl radical through reaction (3), the acetoxy could decompose via reaction (4) to give methyl radical and CO_2 . Examination of the mass 29 TOF



spectrum (shown in figure 8, top) reveals a slow component shown in dotted line due to ethyl radical. The $P(E_T)$ for reaction (3) derived from the mass 29 data using RRKM calculations described below is shown at the bottom of figure 8.

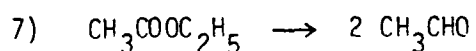
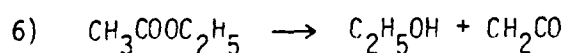
No trace of stable acetoxyl radical could be detected at any mass. Evidently this weakly bound species undergoes complete secondary dissociation either by absorbing additional energy from the CO_2 laser or by being formed above its dissociation limit. The data at mass 15 (from methyl radical) and mass 44 (from CO_2) cannot be fit by a single secondary $P(E_T)$. The methyl radical signal is fit by a $P(E_T)$ averaging over 30 kcal/mol in translational energy and extending beyond 60 kcal/mol. The methyl radical by itself has an average of more than 21 kcal/mol in translation. CO_2 recoiling from methyl radical requires even more translational energy to reproduce the fastest signal (or a heavier particle than CH_3 to recoil from) indicating that a three-body dissociation process is occurring and accounts for at least some of the data. This is reasonable since dissociation of the acetoxyl radical to methyl radical and CO_2 is exothermic by almost 10 kcal/mol and cannot have too high a barrier since the C-C stretching surface has been calculated to be relatively flat.¹⁸

There was no evidence for any other reactions occurring. The results cannot be explained by primary loss of the methyl group, followed by decomposition to give ethyl radical and CO_2 through reaction (5), as this



would produce much faster C_2H_5 product as well as slower methyl radicals.

Simple bond rupture to give CH_3 and CH_3COCH_2 is more endothermic than reaction (3) by at least 5 kcal/mol and should not be important. A theoretical branching ratio calculation described below showed that less than .5 percent should react through this channel. Reactions (6) and (7)



involving hydrogen atom transfer through a four-membered transition state are expected to proceed only with very high barriers, thus limiting their contribution. A reaction analogous to (6) was observed in methyl acetate with a barrier of 69 kcal/mol, but in that case there was no lower energy concerted reaction pathway such as reaction (1). Reaction (7) is a potential source of $m/e = 44$ signal but should also produce signal at $m/e = 43 (C_2H_3O^+)$.¹⁹ Since the $m/e = 43$ data is identical to $m/e = 45$ and different from $m/e = 44$ this channel can be experimentally ruled out.

Branching ratio calculations were carried out to determine the relative contribution from each channel. Using a modification of a method described by Krajnovich,²⁰ the branching ratio between channel A producing fragments of mass m_1 and m_2 , and channel B with fragments m_3 and m_4 , is

$$R\left(\frac{A}{B}\right) = \frac{N(m_1^+, \theta) \cdot \sigma_{ion}(m_3) / m_2 m_3}{N(m_3^+, \theta) \cdot \sigma_{ion}(m_1) / m_1 m_4} \cdot \frac{\int_0^\infty P_B(E_T) \frac{dv_3}{u_3}}{\int_0^\infty P_A(E_T) \frac{dv_1}{u_1}}$$

where $N(m_i^+, \theta)$ is the total number of detected ion counts per laser shot from fragment m_i at angle θ , $\sigma_{ion}(m_i)$ is the ionization cross section, v_i is the lab velocity, and u_i is the c.m. velocity of the neutral m_i . The ionization cross sections were calculated as recommended in ref. 20 using data from the literature.²¹ The integrals represent the expected signal at angle θ and were calculated numerically. Since MPD is isotropic and the laser was unpolarized there are no corrections for the anisotropy.

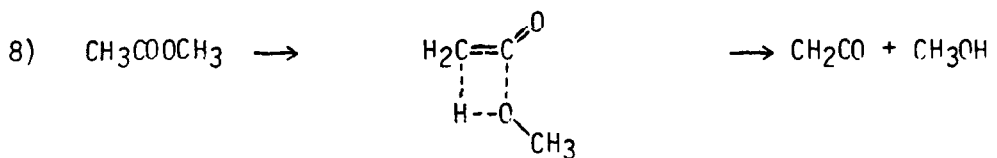
Since data was collected at almost every mass, N_{total} for each fragment was calculated by adding up the total number of ion counts per shot for that fragment at 20°. Minor corrections for the few undetected ions were made by comparison with the methyl acetate data (O^+ , $CHCO^+$) or with known cracking patterns¹⁹ (C_2H^+). All of the data used were obtained under exactly the same experimental conditions, most on the same day, so variations due to laser power, beam intensity, etc., should be minimal.

The ratio between ethylene and acetic acid produced should be unity in the absence of secondary dissociation since these are the two momentum matched fragments from the same dissociation channel. Experimentally these ratios have been within 15 percent of the expected value for cases with no secondary decomposition occurring.^{20,22} In this experiment the ratio was 3.02, indicating that 67 percent of the acetic acid decomposes. Since so much of the acetic acid decomposes it is not surprising that the $P(E_T)$ derived for the surviving acetic acid differs from that of ethylene. The branching ratio between reactions (1) and (3) was calculated to be 33.5 using the data from ethylene and ethyl radical, neither of which undergo secondary decomposition. The fact that 97 percent of the reaction occurs

through the concerted mechanism and only 3 percent by simple bond rupture explains why the latter channel has not been previously observed, and may occur only with the relatively high laser intensities in this experiment or at very high temperatures in thermal studies.

B). Methyl Acetate

Signal from methyl acetate was observed at m/e = 13-16, 28-31, 41, 42, and 44, but not at m/e = 17, 32, 43, or 59. The results are summarized in table 2. As with ethyl acetate, two competing dissociation channels were observed. The large peak at mass 42 (shown in figure 9) was assigned as the parent ion from ketene produced in reaction (8) proceeding through a four-membered cyclic transition state.



The momentum matched methanol fragment was measured at m/e = 31 and is also shown in figure 9. The absence of the parent ion of methanol is not surprising in light of the previous discussion. The $P(E_T)$ which fit both fragments peaks at 19 kcal/mol with an average translational energy release of 21.1 kcal/mol and is shown in figure 10. There was no evidence for secondary dissociation of either fragment.

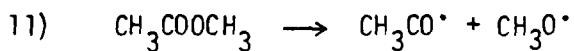
The signal at mass 44, shown in figure 11, top, was explained analogously to ethyl acetate using reactions (9) and (10). Primary





decomposition occurs through a simple bond rupture reaction to produce the acetoxy radical and a methyl radical, then secondary dissociation produces CO_2 and a second methyl radical. The m/e=14 TOF spectrum showing slow methyl radicals from reaction (9), fast methyl radicals from reaction (10), and contributions from reaction (8) is shown in figure 11, bottom.

In addition to the fast peaks from concerted dissociation observed at m/e = 31 and 42 there was a small amount of slower signal in both of these TOF spectra. This signal, which appears at roughly the same time in all the TOF spectra, may be due to dimers or a tiny fraction of the acetoxy radicals which survive to the ionizer (as it is so attributed in figure 9). It could also be due to another dissociation channel such as reaction (11) producing



methoxy and CH_3CO radicals as this channel is no more than 15 kcal/mol more endothermic than reaction (9) and could produce a small fraction of the total signal.²³ In any case this slow signal amounted to less than one percent of the total c.m. frame signal.

As with ethyl acetate, the methyl radical and CO_2 peaks in the secondary dissociation data for the acetoxy radical could be fit reasonably well by a single P(E_T). However, signal from the fast methyl radical was noticeably narrower than would be predicted on the basis of the CO_2 data, indicating that simultaneous three-body dissociation is also occurring

here. The RRKM-style $P(E_T)$ for reaction (9) peaks at zero and releases an average of 3.98 kcal/mol into translation. The $P(E_T)$ for reaction (10) peaks at 15 kcal/mol with an average release of 19 kcal/mol. Both $P(E_T)$ s are shown in figure 12. The fact that we observe essentially the same simple bond rupture channel followed by decomposition of the acetoxyl radical in both ethyl and methyl acetate is further evidence of our correct assignment of this channel.

Calculations similar to those for ethyl acetate were performed to determine the relative contributions of the two dissociation channels. The ratio between methanol and ketene produced in reaction (8) was very close to one, as it should be since neither fragment undergoes secondary decomposition. In the decomposition of methyl acetate, however, the branching ratio between reaction (8) and simple bond rupture, reaction (9), determined using the slow methyl radical data, was 1.16, indicating that simple bond rupture accounts for almost half of the dissociation products, in sharp contrast to ethyl acetate. Since the energy release for reaction (9) is somewhat uncertain (a fairly wide range of $P(E_T)$ s with the same general shape will fit the slow methyl radical data) the branching ratio was checked using the signal from CO_2 . The formula for the branching ratio changes slightly but is essentially the same as that used previously.²⁴ The advantage is that the shape of the c.m. $P(E_T)$ for the CO_2 alone is tightly constrained by the data and the TOF spectra used (at m/e = 16, 28, and 44) are largely uncontaminated by signal from other channels. The signal attributed to CH_3CO_2 was also included, but this affected the calculation by less than 1 percent. The results of this calculation gave a

branching ratio of 1.12, in good agreement with the first calculation. The effect of this branching ratio on the barrier height for concerted reaction is discussed in the next section.

Discussion.

A). Exit Barriers for Concerted Decomposition

RRKM theory is a widely used method for determining rate constants of unimolecular reactions.²⁵ In the case of reactions proceeding without an exit channel barrier (i.e. simple bond rupture reactions) it can be easily extended to predict the translational energy release of the two fragments at a given total energy, simply the amount of energy in the reaction coordinate at the transition state. The resulting $P(E_T)$ peaks at zero and decreases roughly exponentially, in contrast to concerted reactions which are dominated by dynamical effects after the transition state, thus allowing the possibility of large translational energy releases.

We have previously used a further extension of RRKM theory to calculate dissociation barriers for concerted reactions.⁴ This method makes use of the RRKM rate constants for both channels, the branching ratio, and the $P(E_T)$ for the simple bond rupture channel. An MPD rate equation program²⁶ which models absorption, stimulated emission, and dissociation is used to integrate over the duration of the laser pulse and determine how high the molecules are pumped before they dissociate and the relative yield into competing dissociation channels. Since in reactions with no exit barrier, molecules dissociating from a higher level release a higher average amount of translational energy, the absorption cross-section (assumed constant with energy) is varied to match the predicted simple bond rupture

$P(E_T)$ with the experimental one. This provides an internal measure of the energy in the ensemble of dissociating molecules. The barrier height for the competing concerted reaction channel is then varied to produce the correct branching ratio. This process is iterated until both the experimental $P(E_T)$ and the branching ratio are reproduced.

Rate constants and $P(E_T)$'s were calculated using an RRKM program of Hase and Bunker.²⁷ The density of states was calculated from known vibrational frequencies of the ground state, obtained from the literature.²⁸ The transition state vibrational frequencies for calculating the sum of states were estimated by varying some of the ground state frequencies in the transition state in order to reproduce the correct Arrhenius preexponential A-factor. For the simple bond fissions this was taken to be $\log A = 16$, typical for such reactions,⁷ for reaction (1) the literature value of 12.6 was used, and for reaction (8) we used $\log A = 13.9$, in analogy to diethyl ether which also undergoes concerted decomposition through a $\overline{\text{C-C-O-H}}$ four-center transition state to produce ethanol and ethylene.²⁹ All the kinetic parameters used and the calculated results are shown in table 3.

Using ethyl acetate as a test case with $\log A = 16.0$ and a reaction barrier of 80.2 kcal/mol (simply the endothermicity of reaction) for simple bond rupture, $\log A = 12.4$ for the concerted reaction (1), and a branching ratio of 33.5 in favor of reaction (1), an absorption cross-section $7.0 \times 10^{-20} \text{ cm}^2$ was required to give the $P(E_T)$ shown in figure 8. This leads to a reaction barrier of 50 kcal/mol for reaction (1). Converting this to an activation energy⁴ gives a value of 49 kcal/mol at 900°K. This

compares quite favorably with the recommended value of 48.0 kcal/mol in ref. 7 in that temperature range. For methyl acetate, using $\log A = 16.0$ and an activation barrier of 83.4 kcal/mol for the simple bond rupture reaction (9), $\log A = 13.9$ for the concerted reaction (8), and a branching ratio of 1.16 in favor of concerted reaction, we derived a barrier height of 69 kcal/mol and an activation energy of 68 kcal/mol.

Although many approximations were made to derive this value, it is expected to be fairly accurate. This method worked well for ethyl acetate and two nitroalkanes.⁴ The branching ratios here are well determined and should not contribute much error. The RRKM calculations are fortunately rather insensitive to the exact value of the vibrational frequencies as long as they reproduce the A factors correctly. The main uncertainty lies in the kinetic data used, the value of the heat of formation of the acetoxy radical and other species, and the exact shape of the simple bond rupture reaction $P(E_T)$. For the heat of formation of the acetoxy radical, we used a value of -49.6 kcal/mol³⁰ with an uncertainty of ± 1 kcal/mol. The slow methyl radical signal from reaction (8) merges into the signal from other channels near 220 μ sec., so it is difficult to determine how far the $P(E_T)$ for the simple bond rupture channel in methyl acetate extends. The possible influence of three-body dissociation is another potential problem. The fact that the ethyl and methyl radical data from simple bond rupture can be fit with an RRKM-style $P(E_T)$ and the fast methyl radicals and CO_2 can be fit reasonably well assuming a sequential two-body dissociation mechanism argues that three-body effects are not very pronounced, but this point must be taken as an important caveat. We therefore assign a total uncertainty of

±3 kcal/mol to the value of 69 kcal/mol for the barrier to concerted decomposition in methyl acetate. It is heartening to note however, that the activation energy for concerted decomposition of ethyl acetate (which suffers from the same problems) is well within this uncertainty when compared to ref. 7.

B). Dissociation Dynamics

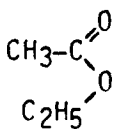
In both ethyl and methyl acetate concerted reactions, a sizable amount of energy is released into translation as the two stable fragments repel each other. It is interesting to compare the translational energy release to the exit channel barrier (obtained by subtracting the endothermicity of the reaction from the activation barrier) which is the energy release after the transition state. For ethyl acetate, the exit barrier is $50.0 - 12.2 = 37.8$ kcal/mol. With an average translational energy release of 21.7 kcal/mol for reaction (1) the fraction of the exit barrier appearing as product translational energy is 57 percent. Methyl acetate has an exit channel barrier of $69.0 - 37.6 = 31.4$ kcal/mol and with an average energy release of 21.1 kcal/mol for reaction (8), 67 percent of the barrier appears in translation. In the secondary dissociation of acetic acid to give ketene and water through a four-center transition state, the exit barrier is about 35 kcal/mol, of which 68 percent becomes translational energy. The results of these and similar experiments have been tabulated elsewhere.³¹

Four and six-center transition states with C, H, and O atoms typically have large translational energy releases,³¹ showing that the exit channel barrier couples strongly with translational rather than internal energy. The considerable excess internal energy above the activation barrier is

distributed randomly and appears mostly as internal energy of the products as evidenced by the relatively small translational energy release in reactions (3) and (9) and other simple bond rupture reactions, which have no exit channel barrier. The large translational energy release from these four and six-center transition states reflects the fact that the transition state occurs "late" on the potential energy surface, and strongly resembles the products. After the transition state, the closed shell products, already close to their equilibrium geometries, experience a strong repulsion due to their overlapping electron clouds, giving rise to the large translational energy release. Using a simple "soft fragment" impulse approximation³² where energy is partitioned between translation and vibration, if an O and an H atom recoil off two C atoms (as occurs in the transition states of both reactions (1) and (8)) 52 percent of the exit channel barrier is predicted to appear in translation for the concerted dissociation of ethyl acetate, and 55 percent for methyl acetate. Including the effects of rotation (difficult to model quantitatively as neither the transition state geometry nor the relative forces between the C-O and C-H pairs are known) would leave even less energy in translation. The fact that significantly more energy is released to translation is further evidence that the fragments are fairly "stiff" as they recoil down the exit channel, and behave as two closed shell fragments which repel each other rather than only the nearest four atoms. In contrast, for an "early" barrier, the transition state more closely resembles the reactants, the products are formed far from their equilibrium geometries and as they relax from the transition state this strain energy becomes product internal excitation, as

apparently occurs with four-center HCl eliminations.³¹

One surprising result was the large amount of translational energy imparted to the dissociation products of the acetoxy radical in reactions (4) and (10). Since the central carbon atom (which ends up in CO₂) changes its hybridization during the reaction, there should be some exit channel barrier, but ref. 18 suggests that it is not much greater than the exothermicity of ~10 kcal/mol. We can think of no convincing reason why more than twice this energy should end up in translation. Another question was why the ethyl or methyl radical from reaction (3) or (9) was so slow if three-body dissociation were occurring. A possible explanation is that in ethyl acetate, concerted reaction occurred when the parent molecule had a geometry similar to the transition state for reaction (1). Simple bond rupture might occur only from geometries with the C₂H₅ and CH₃ moieties on the same side as shown here. Then the C₂H₅ P(E_T) would not



be significantly altered from an RRKM-type exponentially decaying function, but the CO₂ would receive an added little "kick" which would account for its faster than expected translational energy distribution. An analogous process could also be occurring in methyl acetate.

C). Comparison with Previous Results

In both ethyl and methyl acetate decomposition, competition was observed between concerted reaction and simple bond rupture. The branching ratios between the channels shed new light on previous experiments.

Concerted reaction (1) has long been known to be the dominant thermal decomposition pathway for ethyl acetate.⁷ The competing simple bond rupture channel was probably too small to have been observed before. The relatively high laser fluences used in these experiments favor this channel and our higher sensitivity to slow products allowed us to detect this channel for the first time.

For methyl acetate, the concerted reaction has an activation barrier of ~69 kcal/mol while simple bond rupture is ~83 kcal/mol endothermic. Thus, at low temperatures the number of molecules with enough energy to react is small and most of these have below 83 kcal/mol, where they can only undergo concerted reaction. Carlsen et. al. observed only the concerted reaction,¹⁰ finding no evidence for any CH_3CO_2 or CO_2 production. At high temperatures, the A factors determine the relative rates of reaction, thus favoring simple bond rupture which proceeds through a loose transition state and consequently a high A factor. In Sulzmann et. al.'s shock tube experiments, which started at temperatures only slightly higher (1425 K) than the highest in ref. 10 (1404 K), only CO_2 and methyl radicals were observed.¹¹ There are two possible problems with this experiment. The initial (nonequilibrium) shock wave excitation may have produced molecules with an average energy far higher than a temperature of 1425 K would suggest, thus strongly favoring the radical channel. Also, though mass balance was claimed between methyl acetate and both CH_3 and CO_2 , other channels were not explicitly monitored. Using our kinetic parameters or those from ref. 11, the rates for the two channels should have been within a factor of two near 1400 K. At our intermediate to high

energies we saw both channels in about equal amounts, indicating that methyl acetate is probably not a very good source of methyl radicals except at very high temperatures. Furthermore, our experiments indicate that the radical channel is primarily a sequential reaction, with half the methyl radicals being produced translationally cold and half being produced translationally hot, so the use of methyl acetate as a source of methyl radicals for methyl radical reactions should be treated cautiously.

Conclusions.

We have observed competing primary and secondary dissociation channels in the IRMPD of ethyl and methyl acetate. In ethyl acetate, the dominant channel was concerted reaction to give acetic acid and ethylene, with small amounts of simple bond rupture giving acetoxy and ethyl radicals. The acetic acid underwent significant secondary decomposition producing ketene and water. Methyl acetate underwent concerted decomposition forming methanol and ketene and simple bond rupture forming acetoxy and methyl radicals with a branching ratio near unity. All the concerted reactions involved O and H atoms recoiling off of C atoms and released an average of about 20 kcal/mol into translation. Essentially all the acetoxy radicals underwent secondary decomposition to give CH_3 and CO_2 with a surprisingly large release of translational energy.

Using an MPD rate equation model, the activation barrier for the concerted reaction of methyl acetate was determined to be 69 ± 3 kcal/mol assuming an endothermicity of 83.4 kcal/mol for simple bond rupture. All of the concerted reactions (1, 2, and 8) where an H atom is transferred in a cyclic transition state released about 60 percent of the exit channel

barrier into translational energy. This was interpreted in terms of a late transition state after which the closed shell products, formed close to their equilibrium geometries, strongly repel each other. This work is being pursued further to explore the reaction dynamics of different types of transition states.

Acknowledgements.

We would like to thank Xinsheng Zhao for help with computer programming. This work was supported by the Office of Naval Research under Contract No. N00014-83-K-0069.

References.

1. D. S. King, "Infrared Multiphoton Excitation and Dissociation", in Dynamics of the Excited State, K. P. Lawley, Ed. (Wiley, New York, 1982); V. S. Letokhov, Nonlinear Laser Chemistry (Springer-Verlag, Berlin, 1983).
2. I. Oref and B. S. Rabinovitch, Acc. Chem. Res. 12, 166 (1979); M. J. Coggiola, P. A. Schulz, Y. T. Lee, and Y. R. Shen, Phys. Rev. Lett. 38, 17 (1977).
3. Aa. S. Sudbø, P. A. Schulz, Y. R. Shen, and Y. T. Lee, J. Chem. Phys. 69, 2312 (1978); Aa. S. Sudbø, P. A. Schulz, E. R. Grant, Y. R. Shen, and Y. T. Lee, J. Chem. Phys. 70, 912 (1979); F. Huisken, D. Krajnovich, Z. Zhang, Y. R. Shen, and Y. T. Lee, J. Chem. Phys. 78, 3806 (1983).
4. A. M. Wodtke, E. J. Hintsa and Y. T. Lee, J. Phys. Chem. 90, 3549 (1986).
5. P. A. Schulz, Aa. S. Sudbø, D. J. Krajnovich, H. S. Kwok, Y. R. Shen, and Y. T. Lee, Annu. Rev. Phys. Chem. 30, 379 (1979).
6. A. M. Wodtke, E. J. Hintsa, and Y. T. Lee, J. Chem. Phys. 84, 1044 (1986).
7. S. W. Benson and H. E. O'Neal, Kinetic Data on Gas Phase Unimolecular Reactions (NSRDS-NBS 21, U. S. Dept. of Commerce, Washington, DC, 1970).
8. W. C. Danen, W. D. Munslow, and D. W. Setser, J. Am. Chem. Soc. 99, 6961 (1977); R. B. Knott and A. W. Pryor, J. Chem. Phys. 71, 2946 (1979).
9. D. Gutman, W. Braun, and W. Tsang, J. Chem. Phys. 67, 4291 (1977).
10. L. Carlsen, H. Egsgaard, and P. Paasberg, J. Chem. Soc. Perkin Trans. II, 1256 (1981).

11. K. G. P. Sulzmann, D. E. Baxter, M. Khazra, and T.S. Lund, J. Phys. Chem. 89, 3561 (1985).
12. A. M. Wodtke and Y. T. Lee, J. Phys. Chem. 89, 4744 (1985).
13. A. M. Wodtke, Ph. D. Thesis, University of California, Berkeley, 1986.
14. X. Zhao, private communication.
15. Y. T. Lee, "Reactive Scattering: Non-optical Methods", in Atomic and Molecular Beam Methods, G. Scoles and U. Buck, Eds. (Oxford University Press, New York, 1987) and refs. therein.
16. Unpublished results and A. J. Grimley and J. C. Stephenson, J. Chem. Phys. 74, 447 (1981).
17. C. H. Bamford and M. J. S. Dewar, J. Chem. Soc., 2877 (1949).
18. S. D. Peyerimhoff, P. S. Skell, D. D. May, and R. J. Buenker, J. Am. Chem. Soc. 104, 4515 (1982).
19. E. Stenhammar, S. Abrahamsson, and F. W. McLafferty, Atlas of Mass Spectral Data (Wiley, New York, 1969).
20. D. Krajnovich, F. Huisken, Z. Zhang, Y. R. Shen, and Y. T. Lee, J. Chem. Phys. 77, 5977 (1982); D. Krajnovich, Ph. D. Thesis, University of California, Berkeley, 1983.
21. T. M. Miller and B. Bederson, Adv. At. Mol. Phys. 13, 1 (1977).
22. L. J. Butler, Ph. D. Thesis, University of California, Berkeley, 1985, and unpublished results.
23. The difference between ethyl and methyl acetate is that methyl acetate has no low energy concerted reaction channel, almost half the molecules undergo simple bond rupture, and a "small fraction" of this signal in

another channel should be easily visible. In contrast, for ethyl acetate only 3 percent of the molecules undergo simple bond rupture and a small fraction of this will be virtually undetectable.

24. The mass weighting factor becomes $m_1 m_4 / M m_3$ where m_1 is the mass of the single fragment and M is the mass of the reactant molecule.
25. P. J. Robinson and K. A. Holbrook, Unimolecular Reactions (Wiley, New York, 1972).
26. P. A. Schulz, Ph. D. Thesis, University of California, Berkeley, 1979.
27. Available from Quantum Chemistry Program Exchange, Department of Chemistry, University of Indiana, # OCPE-234.
28. T. Shimanouchi, Tables of Molecular Vibrational Frequencies (NSRDS-NBS 39, U. S. Dept. of Commerce, Washington, DC, 1972); B. Nolin and R. N. Jones, Can. J. Chem. 34, 1392 (1956); J. J. Lucier and F. F. Bentley, Spectrochim. Acta 20, 1 (1964); M. A. Raso, M. V. Garcia and J. Morcillo, J. Mol. Struct. 115, 449 (1984).
29. L. J. Butler, R. J. Buss, R. J. Brudzynski, and Y. T. Lee, J. Phys. Chem. 87, 5106 (1983); I. Seres and P. Huhn, Magy. Kem. Poly. 81, 120 (1975).
30. D. F. McMillen and D. M. Golden, Annu. Rev. Phys. Chem. 33, 493 (1982); H. E. O'Neal and S. W. Benson in Free Radicals, vol. II, J. Kochi, Ed. (Wiley, New York, 1973).
31. A. M. Wodtke and Y. T. Lee in Advances in Gas Phase Photochemistry and Kinetics, J. Baggott and M. Ashfold, Eds. (Royal Society of Chemistry, London, 1987).
32. G. E. Busch and K. R. Wilson, J. Chem. Phys. 56, 3626 (1972).

Table 1: MASS SPECTRUM OF IRMPD FRAGMENTS OF $\text{CH}_3\text{COOC}_2\text{H}_5$

Detected ion mass	Neutral fragment	Intensity (ions/laser pulse at 20°)	Reaction channel	Figure
59	CH_3COOH	.013	1	-
45	CH_3COOH	.325	1	3
44	CH_3COOH CO_2	.049 .065	1 4	7
43	CH_3COOH	.402	1	-
42	CH_3COOH CH_2CO	.043 .068	1 2	5
31	CH_3COOH	.030	1	-
30	CH_3COOH	.001	1	-
29	CH_3COOH CH_2CO C_2H_5	.193 .059 .063	1 2 3	8
28	CH_3COOH C_2H_4 C_2H_5 CO_2	.229 .446 .078 .101	1 1 3 4	-
27	C_2H_4 C_2H_5	.680 .015	1 3	-
26	C_2H_4 C_2H_5	.255 .014	1 3	3
18	H_2O	.105	2	5
17	CH_3COOH H_2O	.063 .027	1 2	-
15	CH_3COOH C_2H_5 CH_3	.748 .050 .067	1 3 4	7

Table 1 (cont.)

14	CH ₃ COOH	.196	1
	C ₂ H ₄	.067	1
	CH ₂ CO	.249	2
	C ₂ H ₅	.040	3
	CH ₃	.020	4
13	CH ₃ COOH	.131	1
	C ₂ H ₄	.030	1
	CH ₂ CO	.041	2
	C ₂ H ₅	.029	3
	CH ₃	.009	4

Table 2: MASS SPECTRUM OF IRMPD FRAGMENTS OF $\text{CH}_3\text{COOCH}_3$

Detected ion mass	Neutral fragment	Intensity (ions/laser pulse at 20°)	Reaction channel	Figure
44	CO_2	.571	10	11
42	CH_2CO	.083	8	9
41	CH_2CO	.055	8	-
31	CH_3OH	.104	8	9
30	CH_3OH	.015	8	-
29	CH_2CO CH_3OH	.031 .070	8 8	-
28	CH_2CO CO_2	.080 .297	8 10	-
16	CO_2	.126	10	-
15	CH_3OH CH_3 (primary) CH_3 (secondary)	.109 .339 .301	8 9 10	-
14	CH_2CO CH_3OH CH_3 (primary) CH_3 (secondary)	.281 .012 .394 .159	8 8 9 10	11
13	CH_2CO CH_3OH CH_3 (primary) CH_3 (secondary)	.038 .003 .053 .023	8 8 9 10	-

Table 3: DATA USED FOR REACTION BARRIER CALCULATIONS

Reaction channel	logA	E _A (kcal/mol)	Simple bond rupture P(E _T) used	Reaction barrier (kcal/mol)
Ethyl acetate				
Simple bond rupture	16 ^a			80.2 ^c
Concerted	12.4 ^a	49	fig. 8	50 ^d
Methyl acetate				
Simple bond rupture	16 ^a			83.4 ^c
Concerted	13.9 ^b	68	fig. 12	69 ^d

^aRef. 7.

^bIn analogy to diethyl ether; see text.

^cCalculated using $\Delta H_f^0(\text{CH}_3\text{COOC}_2\text{H}_5) = -103.4 \text{ kcal/mol}$, $\Delta H_f^0(\text{CH}_3\text{CO}_2) = -49.7 \text{ kcal/mol}$, $\Delta H_f^0(\text{C}_2\text{H}_5) = 26.5 \text{ kcal/mol}$, $\Delta H_f^0(\text{CH}_3\text{COOCH}_3) = -98.0 \text{ kcal/mol}$, and $\Delta H_f^0(\text{CH}_3) = 35.1 \text{ kcal/mol}$, taken from refs. 7 and 30, and S. W. Benson, Thermochemical Kinetics (Wiley, New York, 1976).

^dDetermined in this study.

Figure Captions.

- Fig. 1. Energy level diagram showing possible dissociation channels for ethyl acetate. The activation energy for the previously observed channel producing acetic acid and ethylene and all heats of formation were taken from refs. 7 and 30, and S. W. Benson, Thermochemical Kinetics (Wiley, New York, 1976). Both primary channels which we observed are shown in dashed line.
- Fig. 2. Energy level diagram for methyl acetate, similar to fig. 1.
- Fig. 3. TOF spectra of products from reaction (1) at 20°. Data points are represented by open circles in the TOF spectra throughout this paper. Top, ethylene measured at m/e = 26. The large peak is fit by the corresponding $P(E_T)$ shown in fig. 4. The small, slow signal is from C_2H_5 produced in reaction (3). Bottom, acetic acid measured at m/e = 45, fit with a solid line using the lower $P(E_T)$ in fig. 4. The data points and the fit have been lowered to represent the extensive depletion of acetic acid through reaction (2). The dashed line shows an attempt to fit the m/e = 45 spectrum with the $P(E_T)$ derived from the ethylene data. The "missing" signal corresponds to acetic acid which has undergone secondary decomposition. Read text carefully.
- Fig. 4 $P(E_T)$ for reaction (1) derived from the data in fig. 3. The solid line shows the $P(E_T)$ derived from signal due to ethylene. The lower dashed line shows the $P(E_T)$ derived from acetic acid. The crosshatched area represents the acetic acid which underwent

secondary decomposition, and was used as the primary $P(E_T)$ for reaction (2). See text.

Fig. 5 TOF spectra of products from reaction (2) at 20°. Top, CH_2CO^+ from ketene (---), and signal from acetic acid (---) from reaction (1). Bottom, H_2O^+ from water. Fits to the data are from the $P(E_T)$ shown in fig. 6.

Fig. 6 $P(E_T)$ for reaction (2), the secondary decomposition of acetic acid to give ketene and water, derived from the data shown in fig. 5.

Fig. 7 TOF spectra of m/e = 15 and 44 at 20°. Top, methyl radical from reaction (4) (---, fast), acetic acid from reaction (1) (---), and ethyl radical from reaction (3) (****, slow). Bottom, CO_2 from reaction (4) (---) and acetic acid (---).

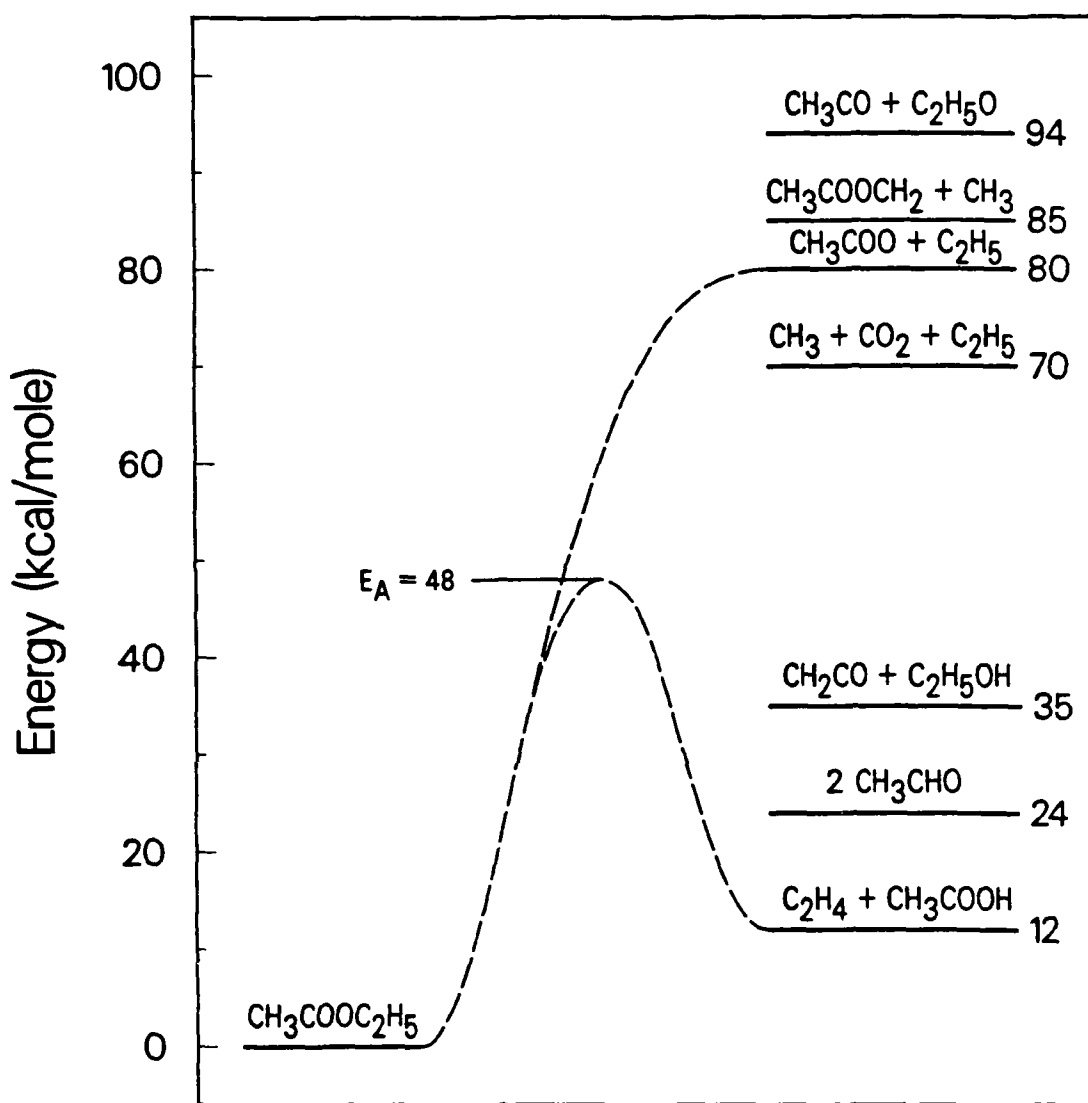
Fig. 8 Top, TOF spectrum of m/e = 29 at 10° showing ketene from reaction (2) (---), acetic acid from reaction (1) (---), and ethyl radical from reaction (3) (****) fit with the $P(E_T)$ shown below. Bottom, $P(E_T)$ for the simple bond rupture reaction (3).

Fig. 9 TOF spectra of the products of reaction (8) at 20°. The large peaks are from ketene (m/e = 42) and methanol (m/e = 31), fit with the $P(E_T)$ shown in fig. 10. The small, slow peaks may be due to surviving acetoxyl radical from reaction (9), and can be fit with the $P(E_T)$ shown in fig. 12, top.

Fig. 10 $P(E_T)$ for reaction (8), derived from the data shown in fig. 9.

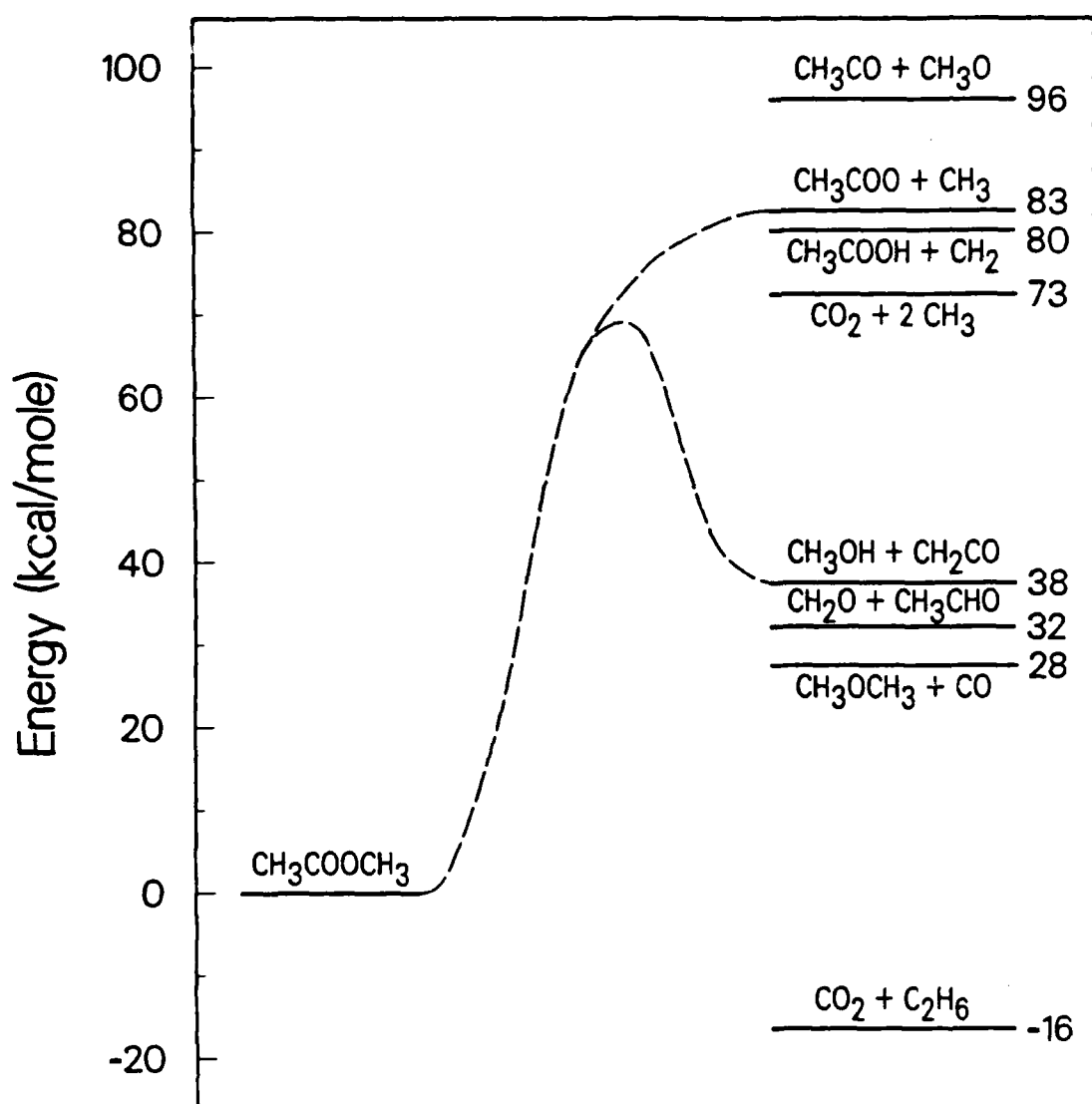
Fig. 11 TOF spectra from MPD of methyl acetate at 20°. Top, CO_2^+ from reaction (10) (---) and possible surviving acetoxy radical from reaction (9) (****). The fits to the data from reactions (9) and (10) are from the $P(E_T)$'s shown in fig. 12. Bottom, CH_2^+ due to fast methyl radical from reaction (10) (---), methanol (-...-) and ketene (—) from reaction (8), and slow methyl radical from reaction (9) (****).

Fig. 12 $P(E_T)$'s for reaction (9), (top), and (10), (bottom), derived in part from data shown in fig. 11.



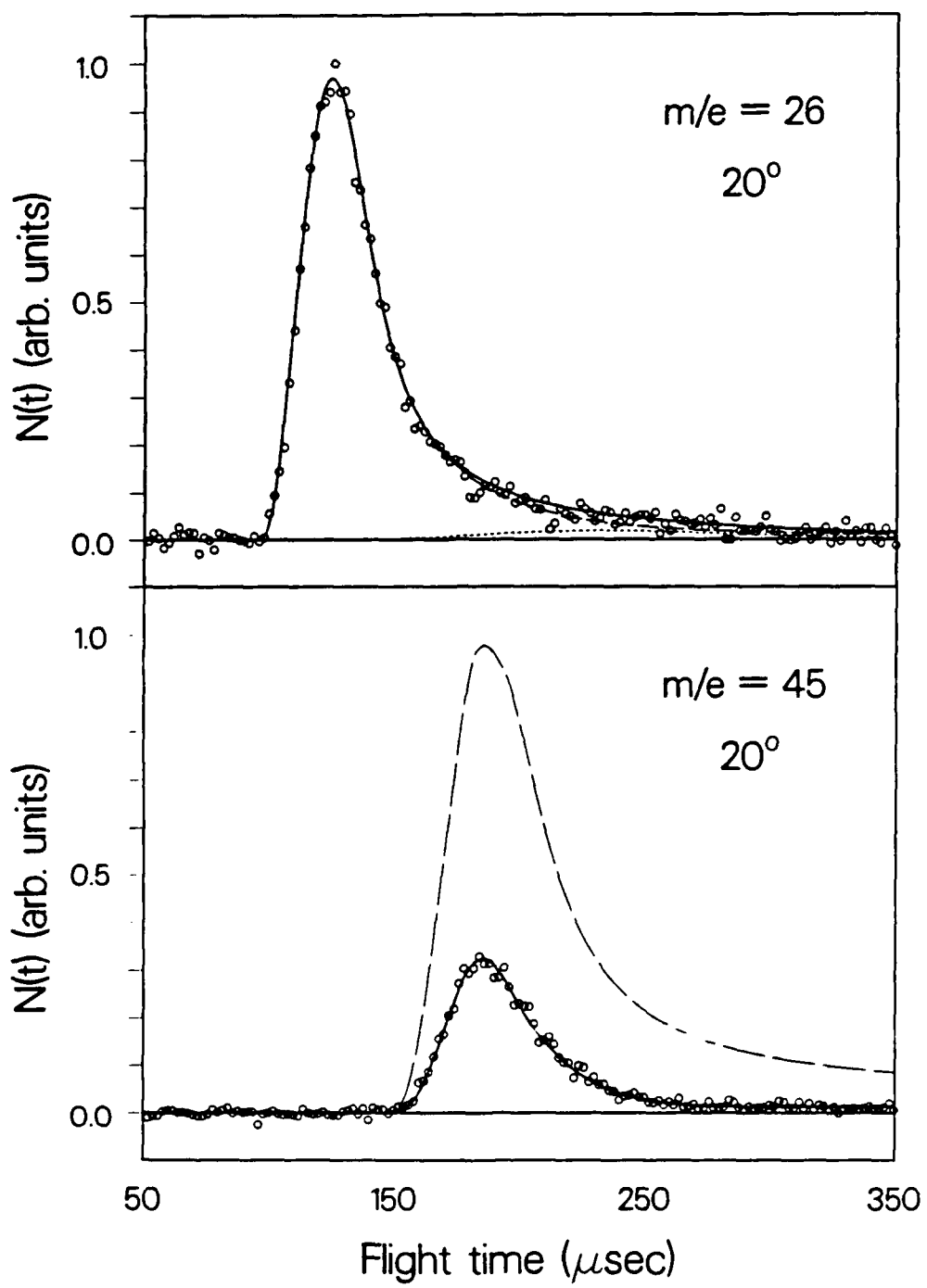
XBL 8711-4548

Fig. 1



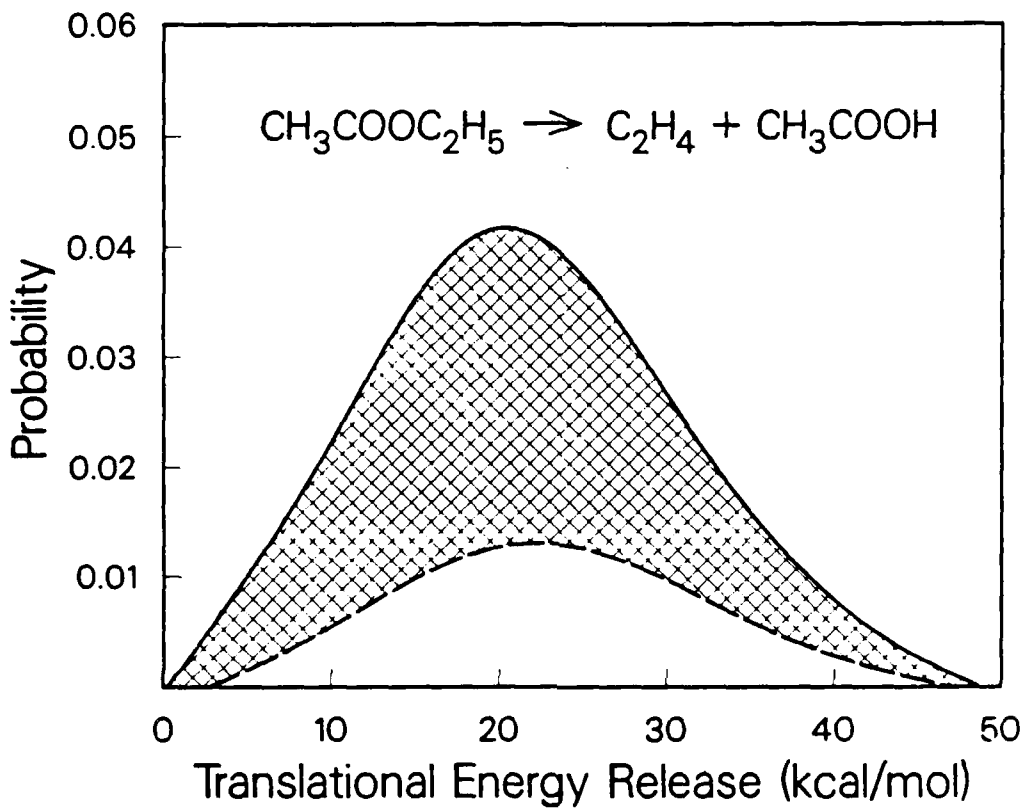
XBL 8711-4549

Fig. 2



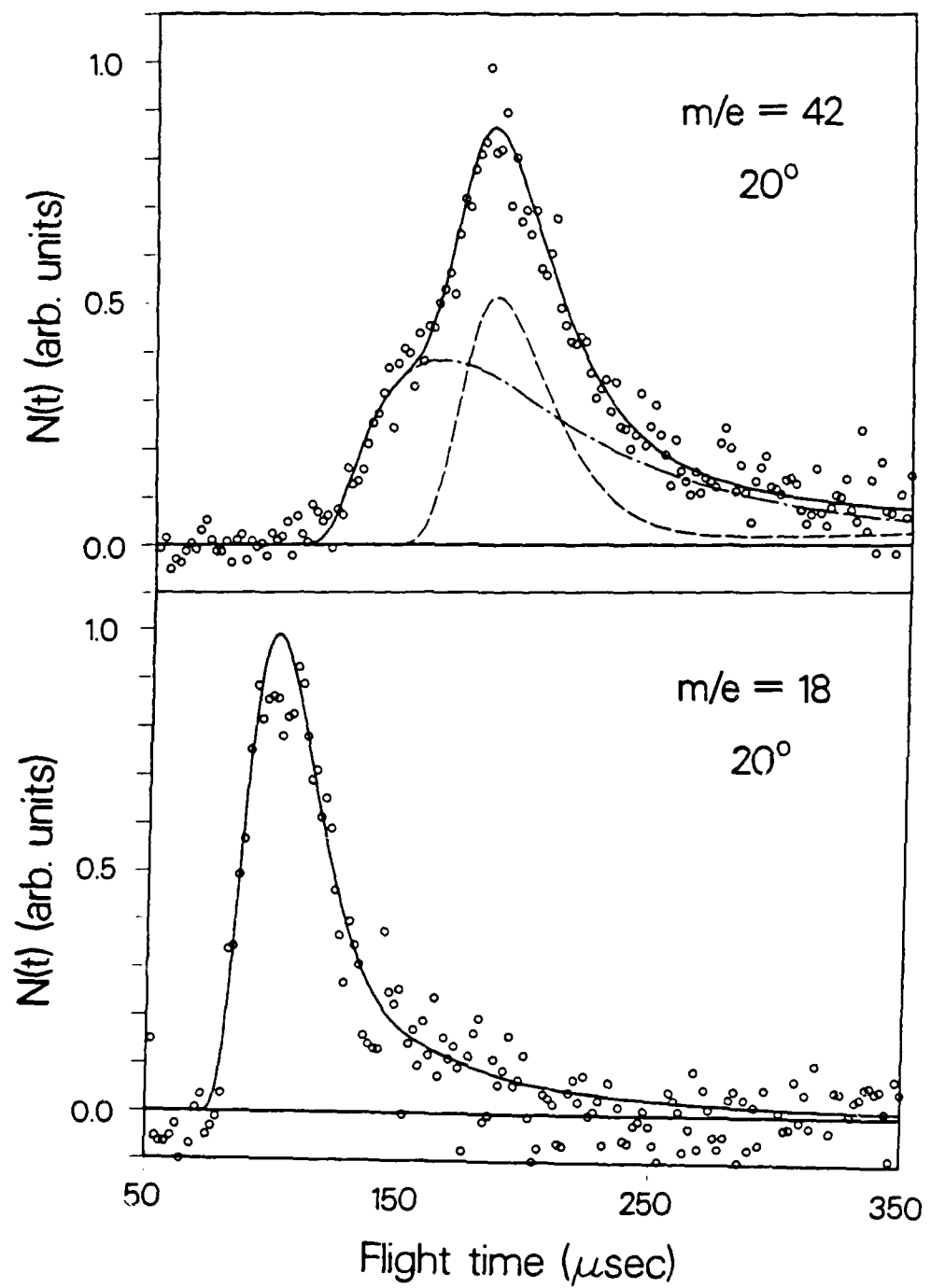
XBL 8711-4541

Fig. 3



XBL 8711-4550

Fig. 4



XBL 8711-4542

Fig. 5

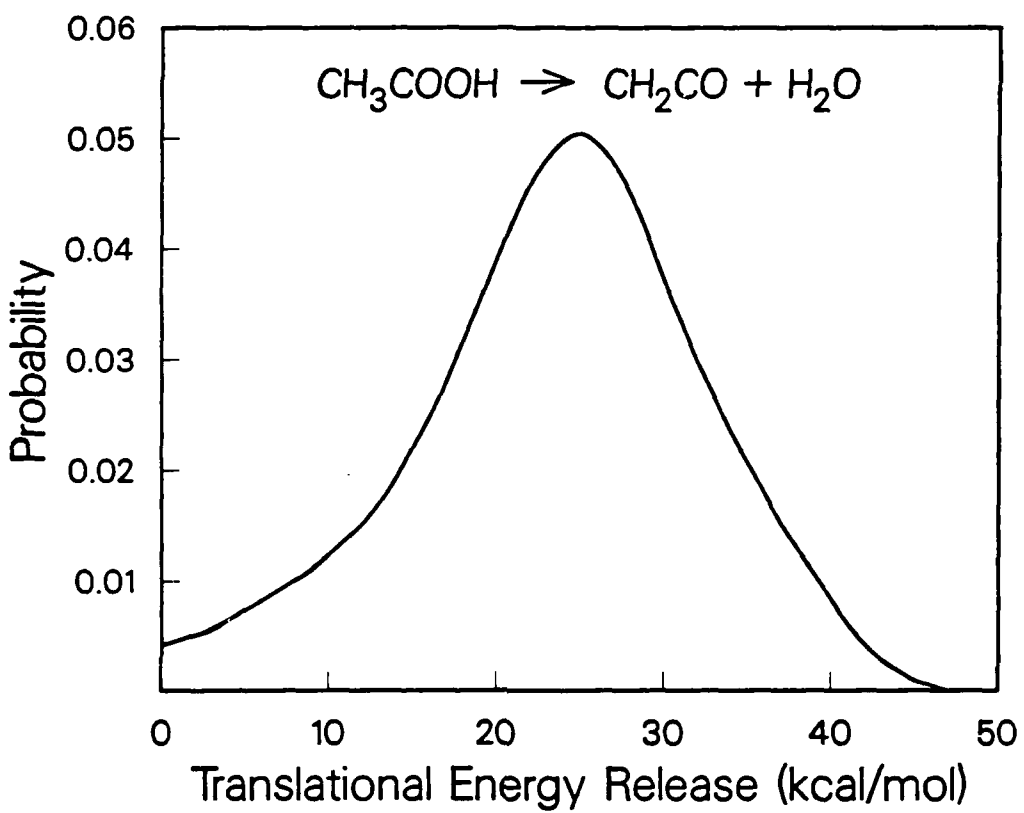
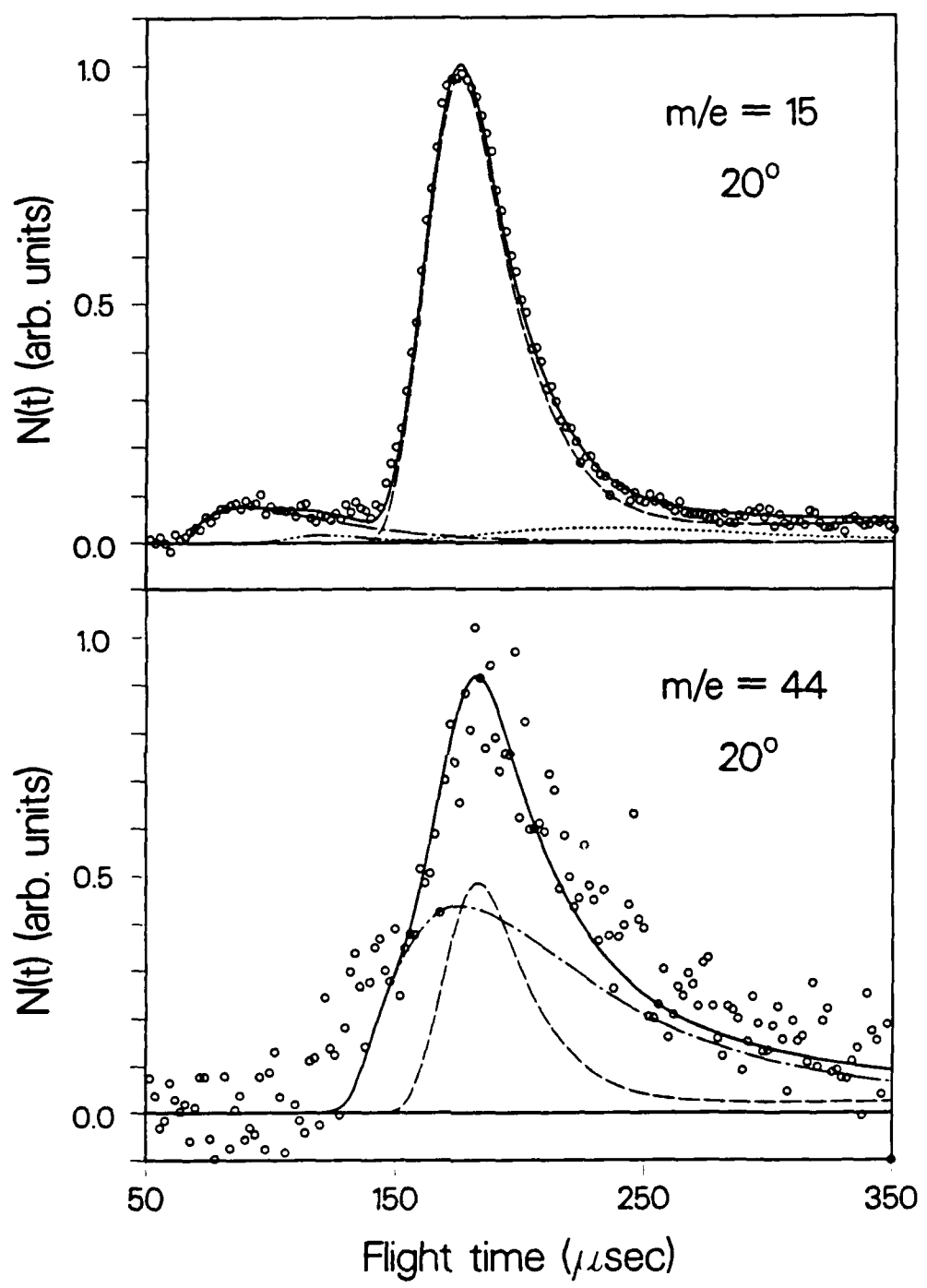
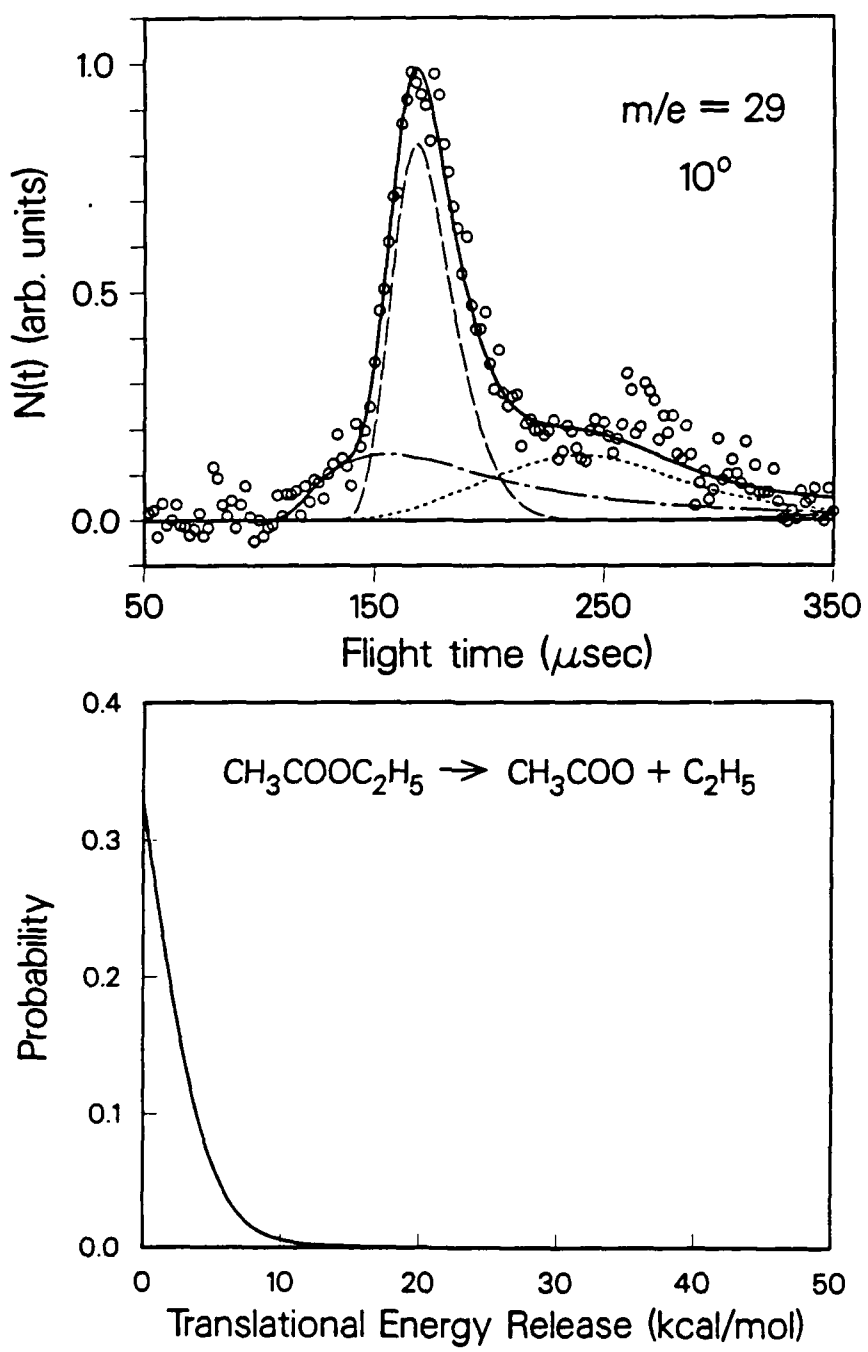


Fig. 6



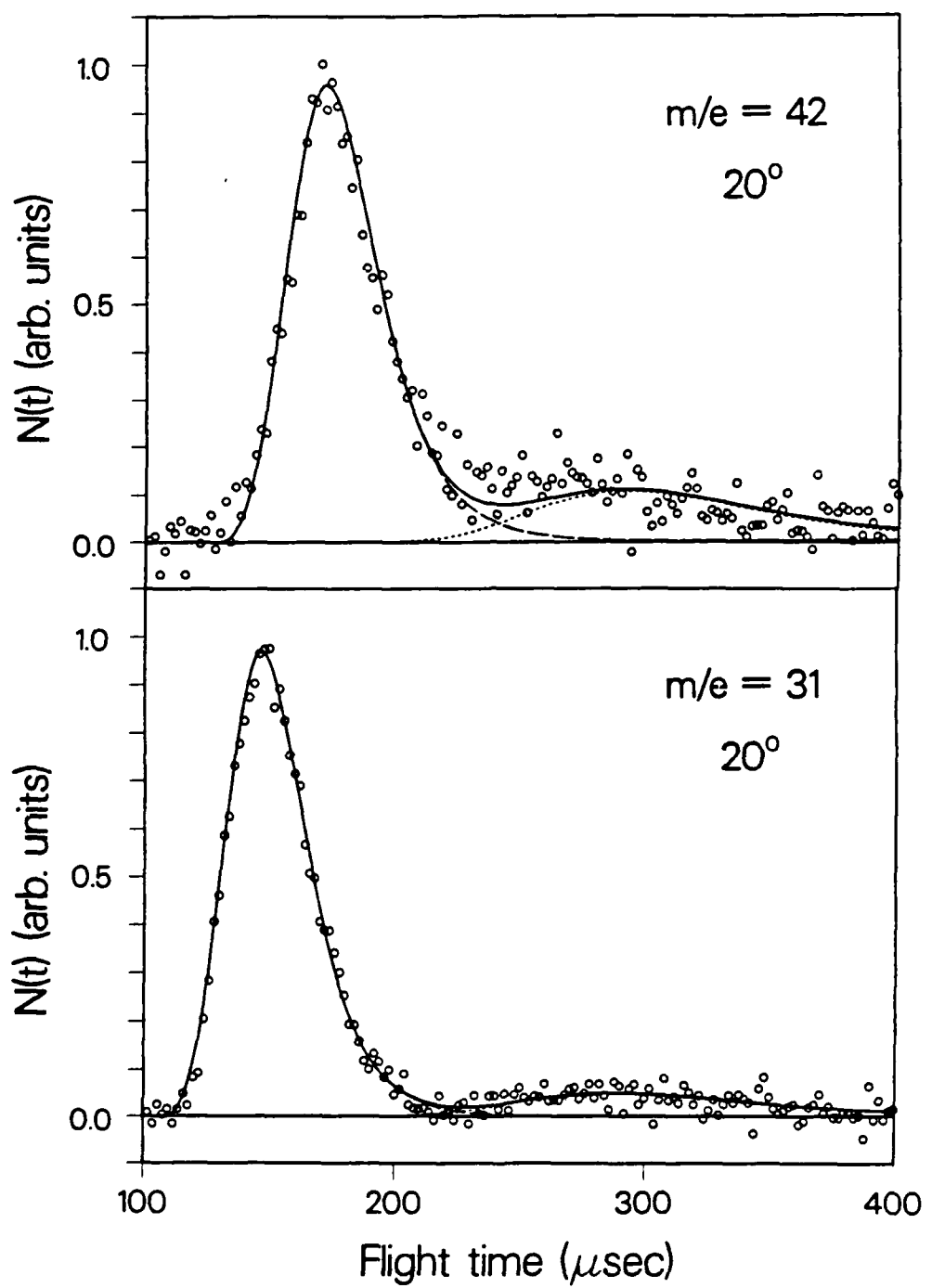
XBL 8711-4543

Fig. 7



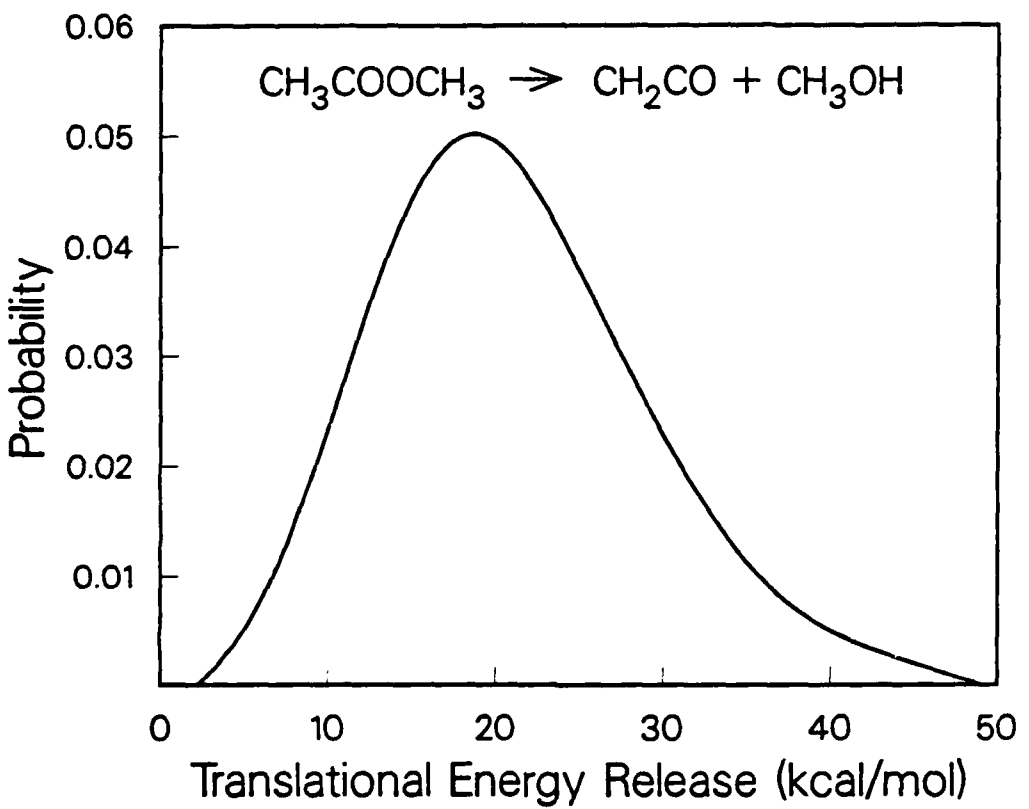
XBL 8711-4544

Fig. 8



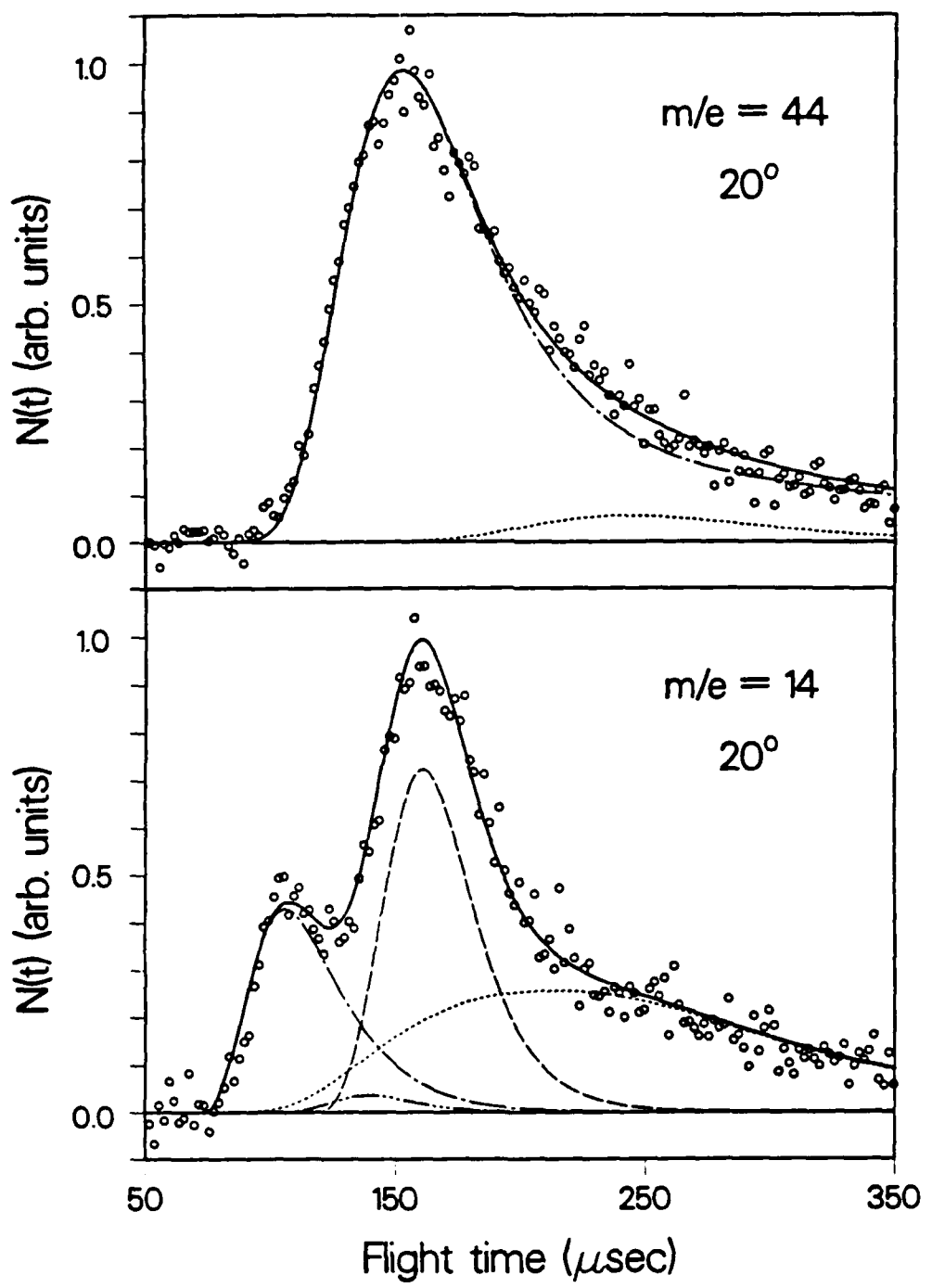
XBL 8711-4545

Fig. 9



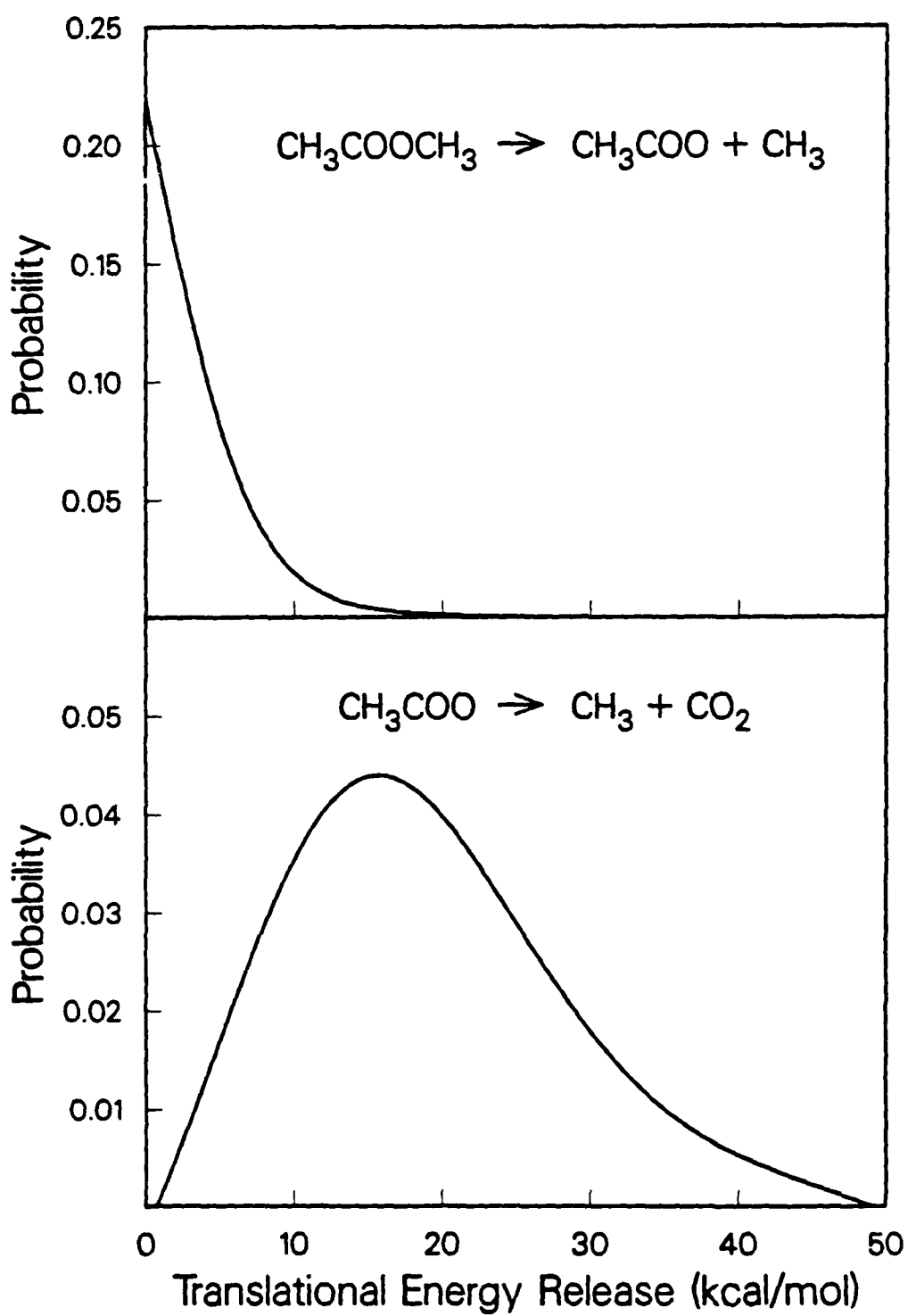
XBL 8711-4552

Fig. 10



XBL 8711-4546

Fig. 11



XBL 8711-4547

Fig. 12